ARTICLE   OPEN

Check for updates

Decoupling of Arctic variability from the North Pacific in a warmer climate

Sharif Jahfer[1], Kyung-Ja Ha [ID][1,2,3,4 ✉], Christian L. E. Franzke[2,3], Sun-Seon Lee [ID][2,5], Keith B. Rodgers[2,5] and Dong-Eun Lee[6]

The sea level pressure variability in the North Pacific modulates the climate of the Arctic and surrounding continents, substantially impacting ecosystems and indigenous communities. Our analysis based on data from the CESM2 Large Ensemble and different Model Intercomparison Project datasets reveals that the interannual variability of Arctic surface air temperature (SAT) gradually decouples from the contemporaneous atmospheric conditions over the North Pacific as external forcing increases in intensity in the future. Future projections show that the North Pacific-Arctic relationship during the fall season consistently weakens in magnitude until the end of this century, and in the 22nd and 23rd centuries, the relationship is negligible throughout the year. We show that under increased greenhouse gas emissions, the regional heat fluxes extensively control the Arctic temperature variability, and the strength of the projected North Pacific-Arctic relationship is strongly dependent on the Arctic sea ice extent. Our results suggest that under future warming, a strong coupling of Arctic SAT with the underlying ocean and a weakening of the meridional pressure gradient driven by an enhanced rate of sea ice retreat will weaken the interannual footprint of North Pacific variability on Arctic SAT. Therefore, we propose that the alarming rate of sea-ice decline over recent decades and projected in the near future could accelerate the rate of decoupling. Further, we suggest that mitigation strategies for the Arctic should focus on regional mechanisms operating on interannual and seasonal timescales.

INTRODUCTION

Observations and modeling studies demonstrate that the Arctic temperature warms at a rapid rate relative to the global mean, with this directing attention to the degree of Arctic Amplification (AA[1–4]). AA is tightly coupled to the changes in the sea ice[5] and the resulting changes in ocean-atmospheric heat exchange[6,7]. With the enhanced rates of sea ice melting, the open ocean areas in the Arctic expand, and the resulting changes in ocean-atmosphere fluxes over the basin thereby play a dominant role in modulating the Arctic air temperature and its variability in the future. Further, these regional changes could affect the interaction of the Arctic with the subtropics.

There is not yet a consensus on the degree of impact of both the rapidly changing Arctic sea ice cover (SIC) and the related strengthening of the AA on the mid-latitudes[8,9]. Using observations and coupled model simulations, it is difficult to isolate the impacts of sea ice loss from warming-induced changes and internal variability[9]. The proposed impacts of rapid Arctic sea ice decline on mid-latitudes include the effect on Eurasian and North American winters[10–13], changes in storm tracks and the strength of the mid-latitude jet streams[14], and increased frequency of extreme events in the mid-latitudes[14,15]. Similarly, climate oscillations over the Pacific and Atlantic Oceans affect the Arctic climate and its variability[16–19].

Arctic sea ice and temperature are known to be modulated by climate variability operating on interannual to multidecadal timescales, including the El Niño Southern Oscillation (ENSO[18]), the Atlantic Multidecadal Variability (AMV[20]), and the Pacific Decadal Variability (PDV[17]). A recent study proposed that the Arctic Oscillation (AO; the dominant mode of sea level pressure

(SLP) variability in the Northern Hemisphere) decouples from the North Atlantic and strengthens its ties with the North Pacific in the projected future climate[19]. This shift in relationship is suggested to be driven by the anomalous future warming of the North Pacific Ocean[19]. Further, the largest decline in SIC in recent decades occurred in the Pacific sector of the Arctic[21]. Another recent study proposes a weakening relationship between wintertime AO and SLP variability over the North Pacific on interdecadal timescales[22]. However, the impact of these changes in the Pacific sector on the covariability of the Arctic SAT with the North Pacific has not yet been well explored.

In the North Pacific, the Aleutian Low (AL) and the North Pacific Oscillation (NPO) are the two leading modes of interannual variability[23,24]. The AL, a semi-permanent low-pressure system centered around the Aleutian Islands, in its positive (negative) phase presents negative (positive) SLP anomalies and cyclonic (anticyclonic) circulation over the North Pacific[25]. The equatorial Pacific Ocean can affect the climate variability of the North Pacific by impacting the strength of AL[18,26]. The strength of AL controls the intrusions of extratropical air into the Arctic, providing a direct link between the tropical and extratropical conditions in the Pacific sector and the polar region[27,28]. The second mode of interannual variability, the NPO, manifests as a see-saw in SLP anomalies between the subtropical and mid-latitude North Pacific[23,24,29]. In their positive (negative) phase, positive (negative) SLP anomalies dominate over the northern subtropical (mid-latitude) Pacific. A recent study concluded that an eastward shift in the zonal mean position of the NPO favors extreme winter SAT over North

[1]Research Center for Climate Sciences, Pusan National University, Busan, Republic of Korea. [2]Center for Climate Physics, Institute for Basic Science, Busan, Republic of Korea. [3]Department of Climate System, Pusan National University, Busan, Republic of Korea. [4]BK21 School of Earth and Environmental Systems, Pusan National University, Busan, Republic of Korea. [5]Pusan National University, Busan, Republic of Korea. [6]Department of Marine Environmental Science, Chungnam National University, Daejeon, Republic of Korea. ✉email: kjha@pusan.ac.kr
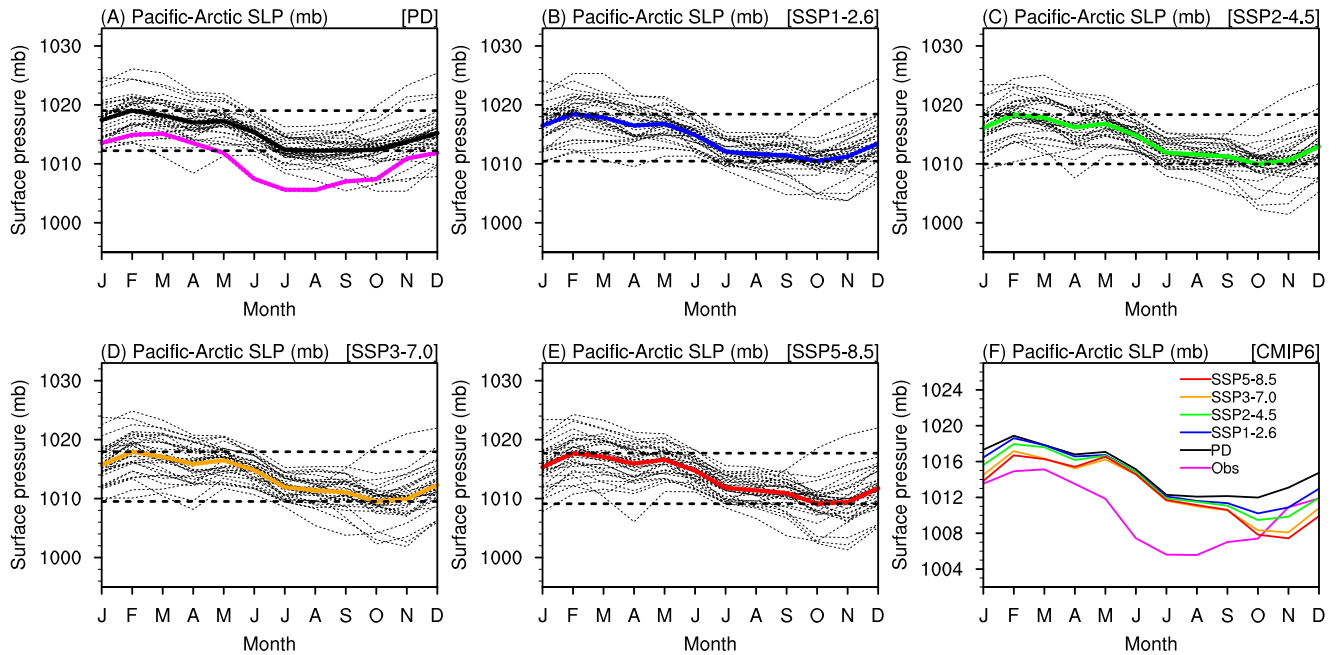
Fig. 1 Annual cycle of sea level pressure (SLP) over the Pacific-Arctic sector. The climatological mean annual cycle of area-weighted SLP (mb) over the Pacific-Arctic sector (70°N–90°N, 90°E–90°W) during the 86 years of historical (1929–2014) and future (2015–2100) periods. **A** The historical annual cycle of SLP from NOAA/CIRES reanalysis (thick magenta curve), 34 CMIP6 climate models (thin black curves), and the corresponding multi-model ensemble mean (thick black curve). **B–E** is the same as (**A**), but for future projections with the multi-model ensemble mean of SSP1-2.6, SSP2-4.5, SSP3-7.0, and SSP5-8.5 represented in thick blue, green, orange, and red curves, respectively. The horizontal dotted lines in (**A–E**) show the CMIP6 ensemble mean of the seasonal peak and trough. **F** Depicts the seasonal cycle of all CMIP6 scenarios used in (**A–E**) for the last 30 years of historical (1985–2014) and future simulations (2071–2100) when the projected SLP change in the Arctic is pronounced.

America[30]. Further, sea ice reduction in the Pacific sector of the Arctic can affect the intensity and phase of NPO[31]. The North Pacific Index (NPI[32]) is defined as the area-weighted average of SLP anomalies over the North Pacific. During the boreal winter, the NPI is strongly correlated with simultaneous AL variability[32] and, therefore, represents the intensity of AL in this study. The NPO in its positive phase corresponds to an enhanced AL and thereby a negative NPI[33]. This study investigates the changes in the interrelationship of North Pacific variability with the Arctic SAT in the projected warming scenario.

Several studies have shown that an intensified AL favors enhanced poleward transport of warmer and wetter air masses, leading to a warmer Arctic and enhanced sea-ice melting[27,28]. This modulation of the Arctic warming rate by North Pacific SLP variability raises the following important questions: (a) How is the relationship between the Arctic SAT and the North Pacific modified in a warmer climate? (b) Will the Arctic SAT become more independent of North Pacific variability in the future? And if so, (c) how long will North Pacific variability remain a significant factor in modulating Arctic SAT? (d) Will regional changes in air-sea fluxes within the Arctic basin overwhelm the effects of remote influences? (e) What are the relative contributions of anthropogenic climate change and internal climate variability in the projected Arctic-Pacific relationship? A motivation for raising these questions is also derived from the fact that a clear understanding of the factors modulating interannual variability in the Arctic will help in the development of long-term adaptation and mitigation strategies. This study attempts to address the above-mentioned questions using reanalysis data, CESM2 Large Ensemble (CESM2LE[34]) output, and individual realizations from the Coupled Model Intercomparison Project Phase 6 (CMIP6[35]).

RESULTS

Projected changes in North Pacific and Arctic surface pressure

The climatological SLP over the Pacific-Arctic sector (70°N–90°N, 90°E–90°W) displays a strong annual cycle with a seasonal high during the boreal winter months of January through March (JFM) and a trough during the summer and fall months (Fig. 1). Though the ensemble mean of the CMIP6 historical simulations (present-day; PD) over 86 years (1929–2014) generally agrees with the NOAA/CIRES reanalysis, the peak-to-trough amplitude is lower (Fig. 1A). Further, while the summer months from June to August mark the observed low in the Arctic SLP, the PD displays an extended seasonal trough spanning from July to October (Fig. 1A). The ensemble mean of seasonal amplitude in the 86 years rises consistently from 6.8 mb in PD to 8.4, 8.5, 9.1, and 9.2 mb in SSP1-2.6, SSP2-4.5, SSP3-7.0, and SSP5-8.5, respectively. Though the projected SLP reduces throughout the year, the reduction during the late fall months and early winter (October through December; OND) is the most pronounced (Fig. 1F), owing to an anomalous decline in the underlying sea ice[36]. In the last 30 years, the projected SLP during OND has deepened by 2.0, 2.7, 4.4, and 5.1 mb in SSP1-2.6, SSP1-2.6, SSP2-4.5, SSP3-7.0, and SSP5-8.5, respectively, compared with the PD (Fig. 1F). The anomalous reduction in SLP during the OND in the projected future increases the seasonal amplitude in the future projections (~ 10 mb in SSP5-8.5) compared to the PD (~ 7 mb). Therefore, the projected mean changes in SLP depict a weakening of high pressure during JFM and a subsequent deepening/reinforcing of low pressure during the OND season over the Pacific-Arctic sector.

The spatial map of the projected response in ensemble mean SLP (evaluated against the PD) during OND reveals a steady decrease in Arctic surface pressure related to the strength of the emission scenario in the last 30 years (Fig. 2[9]). As seen in Fig. 1F, the high emission scenarios SSP3-7.0 and SSP5-8.5 drive the largest reductions in Arctic SLP (Fig. 2D, E). The core of the
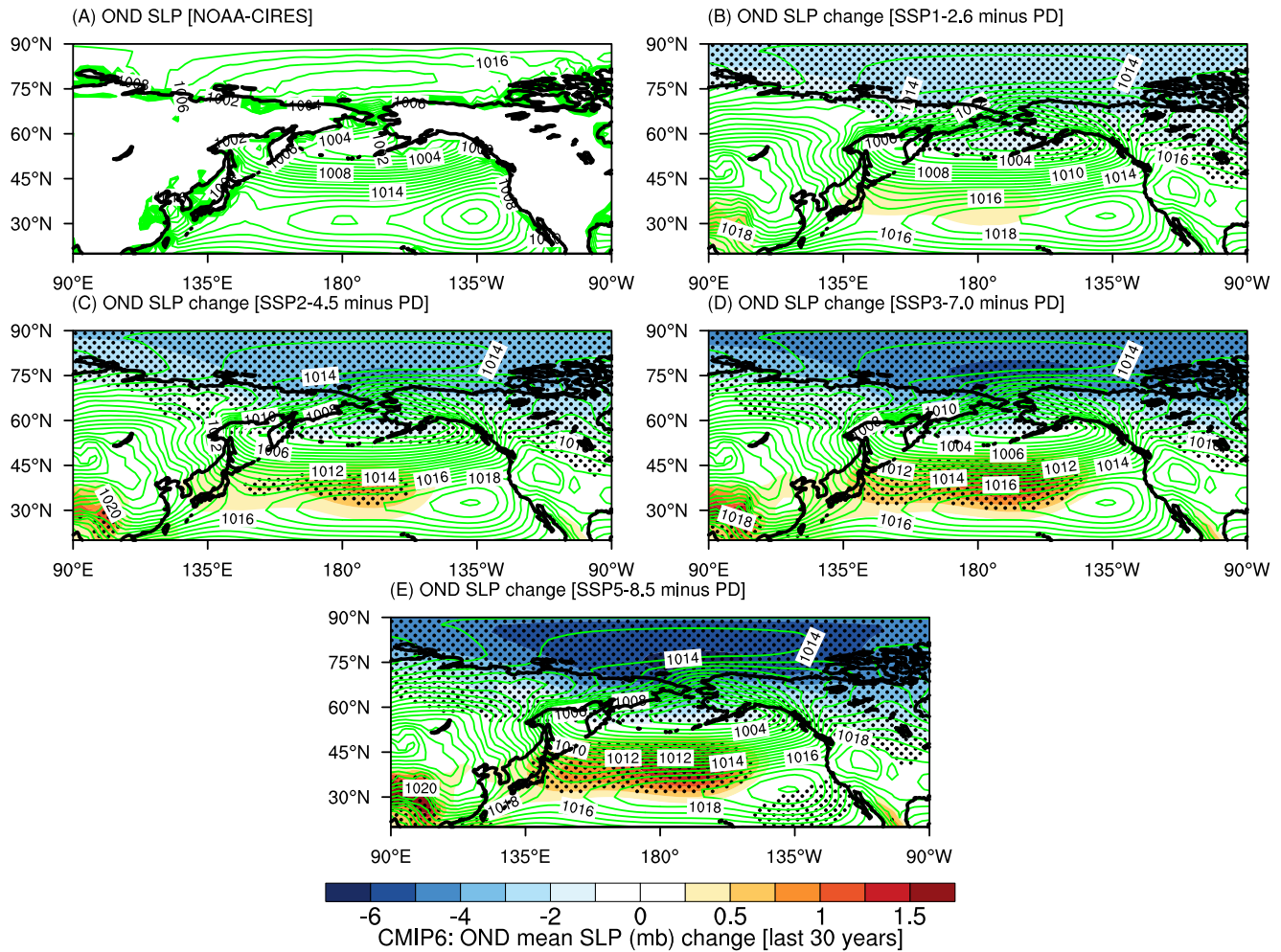
Fig. 2 **Projected changes in sea level pressure. A** The green contour lines show the climatological mean SLP (mb) in the last 30 years of NOAA/CIRES. In (**B–E**), the shades represent the ensemble mean of SLP change in each of the SSP scenarios compared to the PD (SSP minus PD), and the contour lines indicate the climatological mean of OND SLP in the PD during the last 30 years. The anomalies that are statistically significant at 90% confidence level (from a two-tailed T-test) are demarcated by black dots. Note that the label bar scale for the (**B–E**) is not symmetric.

negative SLP difference in SSP3-7.0 and SSP5-8.5 lies poleward of the Bering Strait and is centered around 75°N–80°N, with a maximum reduction of more than 5 mb and 6 mb, respectively. Simultaneously, positive SLP anomalies emerge over the North Pacific Ocean around 30°N–50°N that strengthen in magnitude for higher SSP scenarios. It can be seen that the positive anomalies are weaker than the negative anomalies (note that the color scale bar is not symmetric). Consistent with the CMIP6 simulations, the CESM2LE also captures the projected changes in Arctic SLP in the SSP3-7.0, compared to the PD (Supplementary Fig. 1). However, the magnitude of the SLP increase in SSP3-7.0 over the North Pacific is relatively stronger in CESM2LE than in CMIP6. Therefore, one can expect that the projected changes in the meridional alignment of SLP anomalies during the OND season for both the CMIP6 and CESM2LE simulations could affect the large-scale circulation and atmospheric interactions of the Arctic with the Pacific.

The anomalously low SLP over the Pacific sector of the Arctic in the future projections is primarily driven by changes in the SIC. As the warming-induced retreat in SIC paves the way for an increase in ice-free regions, the open waters absorb incoming radiation during the summer and discharge it during the subsequent cold season when the sea surface temperature (SST) is warmer than the atmosphere above[20]. The warming-related SIC loss peaks during the late summer and fall seasons[37,38], and consequently, the Arctic warming anomalies are pronounced in the cold months of fall and the subsequent winter[5,17]. The magnitude of the SIC reduction (in %) and SAT anomalies strengthen with the increasing intensity of the emission scenario (Supplementary Fig. 2). The maximum SIC reduction in SSP5-8.5 over the last 30 years of the 21st century during OND reaches about 90% along the continental rim of the Arctic, corresponding to an SAT increase of more than 18 °C (Supplementary Fig. 2D). Consistent with previous studies, enhanced loss of SIC reinforces surface warming over the Arctic[39]. The simulated mean SIC in CESM2LE is considerably lower (figure not shown) and could lead to stronger SLP responses (Supplementary Fig. 1B) compared to the CMIP6 counterpart (Fig. 2D). Similar to the OND season, surface warming during JFM is prominent over regions of large SIC loss (Supplementary Fig. 2E–H). Also, consistent with earlier studies, local changes in projected SIC play a more dominant role in anomalous Arctic warming than remote effects[40].

Analysis of surface fluxes of latent and sensible heat reveals that during the OND season, the Arctic basin mean ocean-to-atmosphere heat exchange is enhanced by more than 15 W m^{-2} and 12 W m^{-2}, respectively, under SSP5-8.5 (Supplementary Fig. 3A, B). A similar anomalous increase in ocean-to-atmosphere heat release during the OND season (in response to

anthropogenic forcing) can be found under the SSP3-7.0 scenario used with the CESM2LE (Supplementary Fig. 3B, D). In future projections, the regional SST tends to largely control the variability of the Arctic temperature as a forced response to anthropogenic climate change, especially in the boreal cold months. Therefore, it is evident that the enhanced retreat of sea ice and the resultant changes in surface fluxes primarily drive the anomalous reduction in SLP (Figs. 1, 2, and S1) over the Pacific-Arctic region in future projections[40].

To isolate the role of disparate forcings on the projected changes in the SLP, we used the 21st century simulations under the Detection and Attribution Model Intercomparison Project (DAMIP[41]) based on the SSP2-4.5 pathway. The extension runs for SSP2-4.5 projections driven by various forcings, namely, natural-only (SSP2-4.5-nat), well-mixed greenhouse-gas-only (SSP2-4.5-ghg), and anthropogenic-aerosol-only (SSP2-4.5-aer) are used[41]. Only four climate models were available with the output required for these DAMIP experiments. The ensemble mean of projected SLP anomalies (compared to the PD) under SSP2-4.5 reveals that greenhouse gas forcing contributes the most to the projected reduction in SLP during the cold season (Supplementary Fig. 4A and C). Similar to the responses found under SSP2-4.5, the SSP2-4.5-ghg successfully captures the meridionally oriented dipole pattern of SLP anomalies with a high over the northern Pacific Ocean and a low over the Pacific sector of the Arctic. In contrast, the natural-only and aerosol-only forcings project a positive SLP anomaly over the Arctic owing to higher levels of SIC in SSP2-4.5-nat and SSP2-4.5-aer (Supplementary Fig. 4B and D). While the greenhouse gas-induced warming and subsequent changes in SIC favor a negative SLP anomaly over the Arctic, the aerosol-induced cooling leads to higher SLP (Supplementary Fig. 4C, D).

To ascertain the role of the shrinking Arctic SIC on the development of anomalously low pressure in the Pacific sector of the Arctic, we employ the simulations done for the Polar Amplification Intercomparison Project (PAMIP[42]) as part of CMIP6 (details in Supplementary Information). We use the last 30 years of 100-year PAMIP simulations (2071–2100) constrained by present-day sea-ice extent (pdSIC) and future Arctic sea-ice extent (futArcSIC; Supplementary Fig. 5). The anomalous reduction in SLP in the Pacific sector of the Arctic is well captured in the futArcSIC simulation (Supplementary Fig. 5B). The anomalous meridional SLP anomaly is successfully captured in the experiment with projected sea-ice extent, reaffirming the strong influence of Arctic sea-ice loss on projected SAT and SLP variability. Therefore, it is evident that the sea-ice loss-driven anomalous rise in projected surface temperature drives the low-pressure anomalies in the Pacific-Arctic sector during the cold season, and greenhouse gas forcing is the largest external contributor. Having established this, what are the climatic implications of this Arctic response for future projections? Can it potentially impact the interaction of the Arctic with the Pacific?

## Projected changes in the North Pacific-Arctic relationship

Large-scale variability in atmospheric circulation on interannual to decadal timescales can be represented by the NPI[32]. In this section, we analyze the SAT difference (change in OND SAT compared to the OND SAT during the previous year) corresponding to the contemporaneous NPI difference (area-weighted OND SLP over 20°N–70°N, 120°E–100°W minus OND SLP of the previous year over the same region; see Methods) over the last 30 years of the 21st century, when the Arctic response to external forcing is most pronounced. Studies have shown that the northwest Pacific Ocean exhibits anomalous warming and that SST variability weakens on interannual and decadal timescales, under future warming scenarios[43,44]. These changes in the North Pacific SST could strengthen the AL and its variability. Since the covariability of North Pacific SST with simultaneous Arctic SAT on interannual

timescales is similar to the NPI-related variability, we focus on the relationship between North Pacific SLP and Arctic SAT.

The ensemble mean composite (negative minus positive) of the SAT difference with respect to the sign of the NPI difference under various CMIP6 scenarios is shown in Fig. 3. A negative NPI difference corresponds to a deepening of the AL, and vice versa. Along with the fluctuation in NPI, the SAT over the northern extratropics exhibits strong variability on interannual timescales (Fig. 3). In the PD, during a positive (negative) phase of NPI difference, marking a weakening (deepening) of AL, a zonally oriented bipolar see-saw of SAT bands emerges over the extratropical landmasses, with cooling over eastern Russia and strong warming over the northwestern region of the US and Canada. Simultaneously, Arctic air warms by ~0.4 °C in the PD (Fig. 3A). Compared to the PD, the SAT mean difference over the Arctic increases to ~0.5 °C in SSP1-2.6, but the negative differences are relatively weaker (Fig. 3B). In contrast, under higher SSP forcings, the Arctic SAT differences related to NPI decline with increasing intensity of the external forcing (Fig. 3C–E). The SAT difference is almost absent over the Arctic region in SSP5-8.5. Further, the area-weighted average of warm anomalies over the western part of the North American landmass reduces by more than half with SSP5-8.5, relative to the PD. The spatial distribution of temperature differences corresponding to the NPI index differences simulated by CESM2LE is similar to that of the CMIP6 simulations. Consistent with the CMIP6 simulations, the covariability of Arctic SAT with SLP differences in the North Pacific reduces in the future projections under SSP3-7.0 in CESM2LE (Supplementary Fig. 6). Despite the strong warming trend over the Arctic in the future projections (with a higher magnitude under higher emission scenarios), the NPI-related interannual warm anomalies in the Arctic weaken in a warming climate. Therefore, it can be concluded that the interannual footprint of NPI-related SLP anomalies on Arctic temperature declines steadily over the Pacific sector of the Arctic under future climate change.

The North Pacific-Arctic relationship could be nonstationary, or not fixed in time[45], and the strong decadal variability over the northern high latitudes could affect the interannual relationship. Further, the projected decoupling on interannual timescales happens in the last three decades of the 21st century (when the Arctic SLP reduction is prominent). To understand the relationship under different levels of Arctic sea ice extent for a longer period, model experiments under the Cloud Feedback Model Intercomparison Project (CFMIP[46]), another component of the broader CMIP6 project, in which the models are abruptly forced with multiple levels of pre-industrial CO_2 concentration, were used. This study uses 120 years of output from three CFMIP experiments, namely, abrupt-0.5xCO_2, abrupt-2xCO_2, and abrupt-4xCO_2 simulations in which the pre-industrial CO_2 level is abruptly halved, doubled, and quadrupled, respectively. While abrupt halving of CO_2 (abrupt-0.5xCO_2) resulted in a strong NPI-related warming over the Arctic averaged over 120 years, the corresponding SAT changes in the abrupt-2xCO_2 and abrupt-4xCO_2 weakened considerably (Supplementary Figure 7). Note that under abrupt halving (quadrupling) of CO_2, the Arctic sea ice extent increases (completely disappears) within a decade (figure not shown). Therefore, the gradual weakening of NPI-related SAT warming in the Arctic with increasing CO_2 levels (Supplementary Fig. 7) confirms our finding that the North Pacific-Arctic relationship diminishes in a warmer climate and that the extent of sea ice is a crucial factor in determining the intensity of the teleconnection.

Over the last 30 years of the CMIP6 SSP scenarios (2071–2100), some of the climate models have had significant SIC in the Pacific sector of the Arctic (not shown). We use CMIP6-ext simulations (under SSP1-2.6 and SSP5-8.5 scenarios) to analyze the relationship during the 22nd and 23rd centuries, by which time the SIC is completely absent in SSP5-8.5. The ensemble mean of the SAT difference in the 165 years of historical [1850–2014] and future
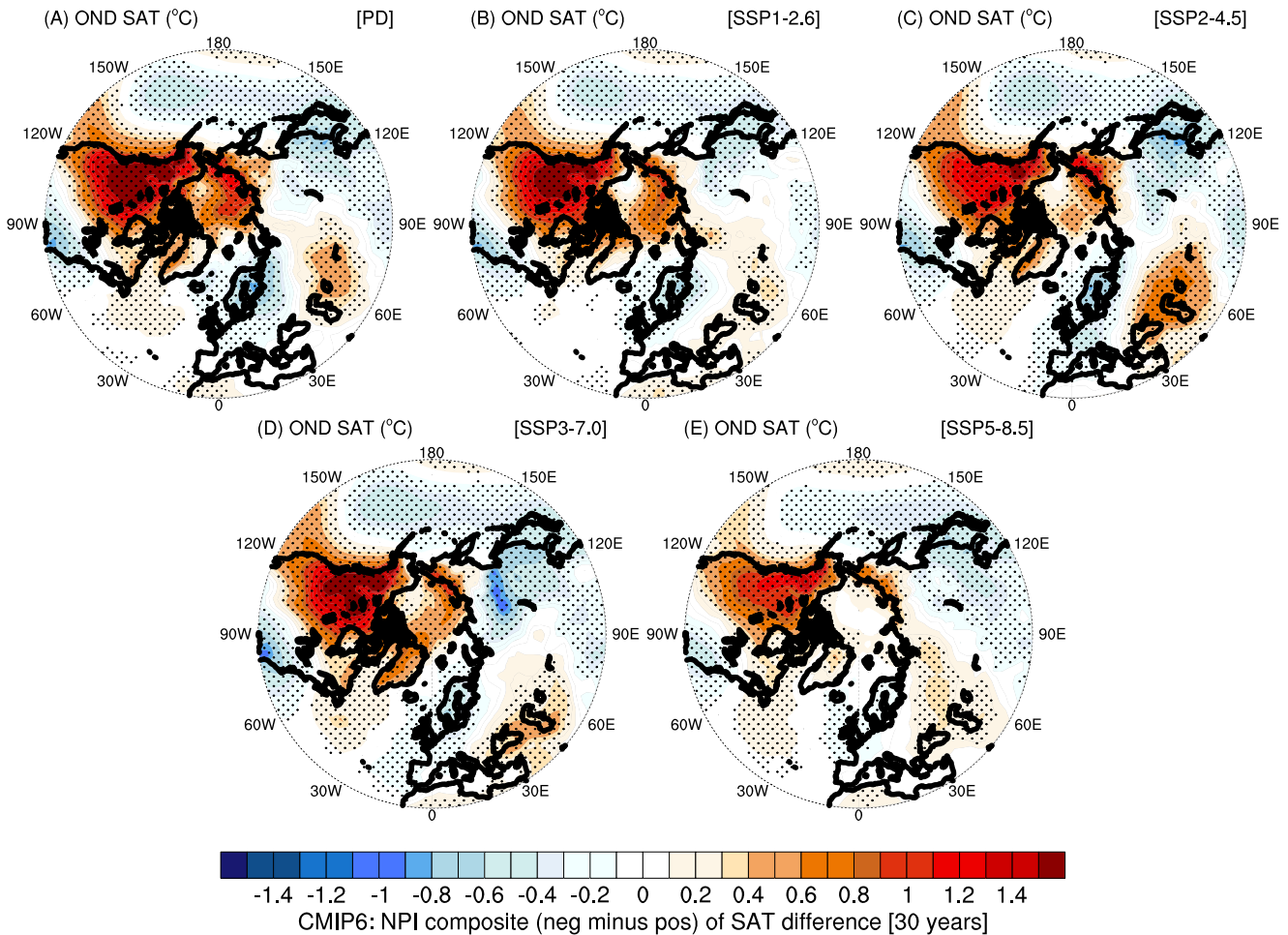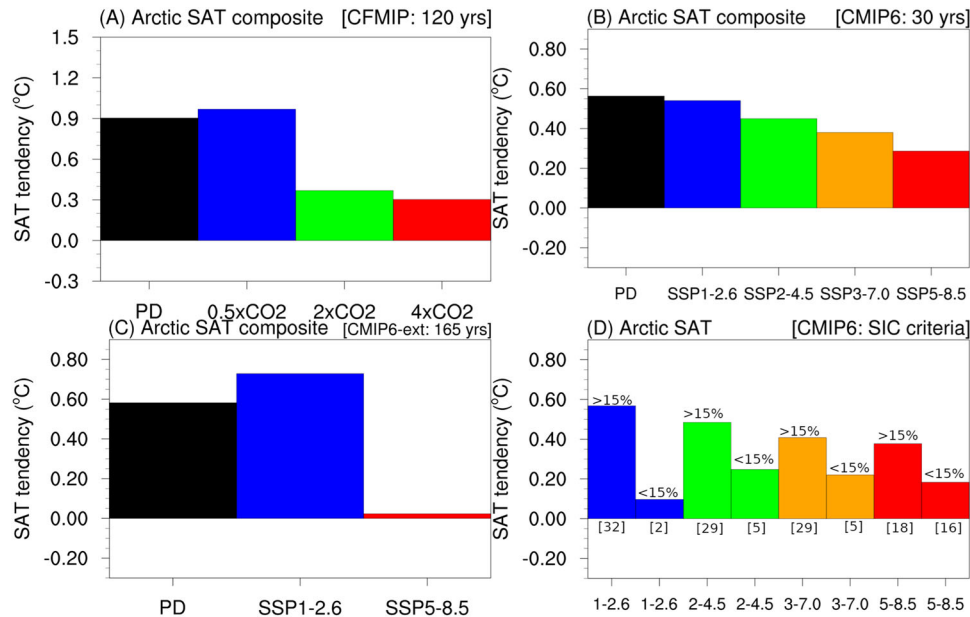
Fig. 3 Composite of NPI-related surface air temperature (SAT) difference in CMIP6. Composite (negative minus positive) of ensemble mean SAT (°C) difference during OND (relative to OND SAT of the previous year) with respect to contemporaneous North Pacific Index (NPI; SLP area-weighted average over 20°N–70°N, 120°E–100°W) difference in the last 30 years of the historical and future simulations. **A** PD, (**B**) SSP1-2.6, (**C**) SSP2-4.5, (**D**) SSP3-7.0, and (**E**) SSP5-8.5, respectively. The changes that are statistically significant at 90% confidence level are demarcated by black dots.

[2136–2300] scenarios shows that the contemporaneous covariability of North Pacific SLP and Arctic SAT is strong under PD conditions and an SSP1-2.6 projection (Supplementary Fig. 8A, B). As expected, the footprint of North Pacific variability during OND is negligible over the Arctic under the SSP5-8.5 scenario (Supplementary Fig. 8C). The ensemble mean evolution of the SAT composite (corresponding to a negative minus positive NPI difference) reveals that under the high forcing scenario of SSP5-8.5, the surface air warming related to SLP deepening over the North Pacific gradually decreases until the end of the 21st century (Supplementary Fig. 9C). In the 22nd and 23rd centuries, the Arctic SAT response to the North Pacific SLP under SSP5-8.5 becomes negligible relative to the PD and SSP1-2.6 cases (Supplementary Fig. 9). The mean NPI-related warming of ~0.6 °C over the period of 2015–2300 suggests that the projected relationship is maintained in the 22nd and 23rd centuries under weaker external forcing and in the presence of sea ice (Supplementary Fig. 9B).

A comparison of the magnitude of the SAT difference over the Arctic with respect to the North Pacific SLP variability underlines our finding that under strong external forcing that results in considerable sea ice loss, the relationship declines during the fall season (Fig. 4). In the abrupt-0.5xCO2 experiment, the Arctic surface air changes by more than 0.7 °C with AL variability (averaged over 120 years; Fig. 4A). Similarly, in the last 30 years of the CMIP6 scenarios, the ensemble mean NPI-related SAT

variability weakens progressively with an increase in forcing (it drops by ~50% in SSP5-8.5 compared to PD; Fig. 4B). The decoupling is pronounced in the extended future simulations (CMIP6-ext; 165 years [2136–2300]) of SSP5-8.5 where the mean SAT change is negligible and SIC has completely vanished in the Arctic (Fig. 4C). In the CMIP6 projections, the simulated SIC varies considerably among the 34 climate models used in the study. We find that in the models with less than 15% SIC cover in the last 30 years of the 21st century, the SAT covariability with the North Pacific reduces by more than 50% under all SSP simulations (Fig. 4D). Therefore, it is evident that the Arctic decouples from the simultaneous North Pacific variability during the fall months, and the strength of the dissociation is dependent on the SIC in the Pacific sector of the Arctic. Further, in the extended future (beyond 2100), the Arctic SAT variability will become nearly independent of the North Pacific variability.

The annual cycle of SAT change with the simultaneous North Pacific SLP variability shows that the weakening of the covariability under high emission scenarios is evident during the fall (Supplementary Fig. 10). The ensemble mean SAT variability drops from ~1.0 °C in the PD and SSP1-2.6 to about 0.1 °C under the SSP5-8.5 scenario during the fall and winter months (Supplementary Fig. 10B). We find that the decoupling under the SSP5-8.5 scenario, limited to the OND season in CMIP6, extends to the winter months in the extended future (2136–2300) when the sea

Fig. 4 Projected changes in NPI-related surface air temperature (SAT). The ensemble mean of the composite (negative minus positive) of NPI-related SAT difference averaged over the Arctic (70°N–90°N, 90°E–90°W) during the OND season in various CMIP6-endorsed MIPs is shown. **A** SAT difference averaged over 120 years of the PD, abrupt-0.5xCO2, abrupt-2xCO2, and abrupt-4xCO2 are represented by black, blue, green, and red bars, respectively. **B** CMIP6 [30 years], (**C**) 165 years of extended CMIP6 projections for the period 2136–2300, and (**D**) composite of SAT difference in CMIP6 climate models with SIC percentages of <15% and >15% under each of the projected scenarios. In (**D**), the number of models classified based on 15% SIC criterion is given in square brackets.

ice is completely absent in the Arctic (Supplementary Fig. 10B). However, in the last 30 years of CMIP6 simulations, the SIC over the Arctic has been significant during the winter months, and therefore the relationship of the Arctic SAT with the simultaneous North Pacific SLP has been maintained (Supplementary Fig. 10A).

The North Pacific-Arctic interannual relationship in the projected future can be affected by a strong weakening of either the NPI or the Arctic SAT. The interannual variability of the NPI difference (shown as SD) is ~1.0 mb in the first and last 30 years of the CMIP6 and CMIP6-ext simulations and therefore exhibits no significant trend (Supplementary Fig. 11A, B). But the variability of the Arctic SAT difference decreased during the last 30 years of the CMIP6 and CMIP6-ext simulations (Supplementary Fig. 11C, D). Though the SD of Arctic SAT in other SSP scenarios also shows a decrease in the last 30 years, the greater loss of sea ice under SSP5-8.5 resulted in a strong weakening of SAT variability. Under the SSP5-8.5 during the extended future period, the Arctic SAT variability drops from ~1.5 °C to ~0.5 °C (Supplementary Fig. 11D). This strong reduction in variability could considerably affect the interaction with the extratropical Pacific. To quantify the relative contribution of North Pacific SLP variability to the Arctic SAT, we find the fraction of SAT variability linked to the North Pacific (NPI-related Arctic SAT difference divided by the Arctic SAT variability). In the CMIP6 simulations, under SSP5-8.5, the ensemble mean fraction of NPI-related SAT difference drops from 0.38 during the first 30 years to 0.26 during the last 30 years. In the extended simulations, the fraction of NPI-related SAT change drops to ~0.1 in the last 30 years of SSP5-8.5 (Supplementary Fig. 11F). Therefore, it can be stated that even under a strong weakening of SAT variability in the absence of sea ice under the high SSP scenario, the contribution of the North Pacific reduces to about one-fourth (75%) in the extended future. Hence, our claim of a weakening of the contemporaneous North Pacific-Arctic relationship under a high emission scenario in the projected future holds true.

To quantify the impact of the Arctic SAT response to NPI under different scenarios, we regressed the OND SAT difference onto the contemporaneous NPI difference simulated by CMIP6-ext (Supplementary Fig. 12). The ensemble mean of the regression shows that the Arctic SAT covaries strongly with the NPI under PD and SSP1-2.6 scenarios, with a maximum change of more than 0.7 °C (Supplementary Fig. 12A, B). However, in the extended future, the Arctic response to the North Pacific will be considerably weaker, with negligible change over the Arctic Ocean (Supplementary Fig. 12C). Therefore, we can state that under SSP5-8.5, the Arctic SAT variability decouples from the North Pacific in the absence of sea ice.

DISCUSSION
The SLP variability over the North Pacific modulates the interannual variability of surface temperatures over the northern extratropics. Here we use reanalysis data and climate model simulations available through CMIP6 as well as the CESM2LE to demonstrate that the linkage between contemporaneous atmospheric variability in the North Pacific and Arctic SAT weakens considerably under stronger warming scenarios. Owing to the drastic retreat of sea ice during the fall season, open water is able to heat the overlying air when the SAT is cooler. During the last three decades of the 21st century, the simulated anomalous retreat of sea ice resulted in a projected higher rate of warming. Consequently, SLP over the Pacific sector of the Arctic lowers by more than 5 mb under the strongest scenario (SSP5-8.5) leading to the development of an anomalous meridional SLP gradient between the North Pacific and the Arctic. The anomalous meridional gradient in SLP could affect large-scale circulation. The weakening of the projected interaction between the Arctic and the simultaneous atmospheric conditions in the North Pacific is reflected in changes in the 850 mb wind pattern (Supplementary Fig. 13). Climatologically, the wind anomalies over the North Pacific during a deepening of AL (negative NPI) exhibit strong clockwise circulation to north of 40°N. The difference (SSP minus PD) in the negative NPI-related difference of the u and v components shows that the variability of large-scale circulation

in the North Pacific weakens under high SSP scenarios (Supplementary Fig. 13). The anomalous clockwise circulation in the SSP5-8.5 depicts a strong weakening of NPI influence on low-level circulation (Supplementary Fig. 13D). The weakening of NPI-related circulation in the North Pacific could eventually weaken the interaction of the North Pacific with the Arctic.

To understand the central role of sea ice, we analyzed the abrupt-CO_2 experiments with 0.5×, 2×, and 4× times pre-industrial CO_2 levels available for a period spanning 150 years (Supplementary Fig. 14). In the presence (absence) of sea ice, the interannual variability of Arctic temperature is tightly (weakly) coupled to North Pacific SLP variability (centered around the AL region) in the abrupt-0.5xCO_2 (abrupt-4xCO_2) experiments (Supplementary Fig. 14B and D). The key region of interannual SLP variability associated with the Arctic SAT shifts gradually from over the North Pacific (centered around 55°N) in the abrupt-0.5xCO_2 to over the Arctic (centered around 75°N) in the abrupt-4xCO_2 experiment (Supplementary Fig. 14B and D). The role of greenhouse forcing in this decoupling is evident in the SSP2-4.5 DAMIP experiments with disparate forcings (Supplementary Fig. 15). The dominant relationship of the Arctic SAT with SLP shifts from the North Pacific in the PD to the Arctic in the greenhouse-only forcing scenario (Supplementary Fig. 15C).

Our analysis shows that atmospheric conditions over the North Pacific affect the contemporaneous Arctic SAT in the presence of sea ice and small external forcing. With an increase in intensity, as seen in the extended future simulations (Supplementary Fig. 9), the relationship gradually indicates dissociation. The increased surface ocean warming also plays a dominant role in the projected decoupling. Climatologically, in the Pacific sector of the Arctic, the surface ocean is covered by sea ice during the winter and the late fall months during the historical period. However, during the summer months, the sea ice melts and open water absorbs the incoming solar radiation, warming the surface ocean. The heat stored in the upper ocean during the summer is released into the atmosphere during the fall and winter months, when the atmosphere above is cooler. Therefore, in the PD, the SAT variability over the Arctic during the OND is strongly coupled to the summertime SST (maximum during the JAS season; Supplementary Fig. 16A). During the OND, the SST influence on the SAT is minimal as the SIC regrows in the Arctic in the PD. In contrast, under SSP5-8.5 and SSP3-7.0 scenarios, the surface ocean has been relatively ice-free in the Pacific sector in the last 30 years, and therefore, the OND SAT variability over the Arctic region becomes increasingly coupled to the SST variability (Supplementary Fig. 16). The strong coupling of SAT and underlying SST during OND is more evident in the extended CMIP6 simulation under SSP5-8.5 (Supplementary Fig. 16B).

Studies linking regional Arctic warming with faraway tropical regions[47] have raised concerns about the increasing role of remote natural variability in a warming climate[48]. This study shows that the strong relationship between the Arctic and the contemporaneous atmospheric conditions over the North Pacific declines considerably under SSP5-8.5 forcing. This is an indication that the Arctic climate will evolve to become relatively independent of extratropical variability under the projected high emissions scenario. Our analysis reveals that internal variability as well as forced perturbations contribute to a projected dissociation of Arctic variability from North Pacific variability. This could be a manifestation of the adjustments to the Arctic sea ice retreat. The principal regions of variability in sea ice-driven Arctic SAT under SSP3-7.0 and SSP5-8.5 scenarios retreat to the central Arctic region, eventually leading to a decoupling of Arctic variability from the North Pacific. The dissociation of the relationship holds true over the 150-year duration of the abrupt-2xCO_2 and abruptx4CO_2 perturbations. This suggests that in the extended future (22nd and 23rd centuries), when the sea-ice extent is minimal, the regional air-sea fluxes will take over the

control of the winter-time Arctic SAT and its variability. Further, anthropogenic-related anomalous warming over the Arctic (AA) could considerably lower the meridional temperature gradient and thereby the interaction between the Arctic and the lower latitudes[49,50]. Therefore, the projected future weakening of low-level wind anomalies related to the NPI index in the Pacific-Arctic sector and the reinforced role of underlying warm Arctic SST on SAT could reduce the projected subtropical impact on Arctic SAT variability during the cold season.

In summary, our results show that the natural and forced variability of the North Pacific will have a relatively weaker role in the Arctic SAT variability in the future. Our results are important especially when the Arctic is warming at an anomalously high rate and its impact on climate extreme events such as increased frequency of extreme events[14,15] intensification of marine heatwaves[51]. The results imply that future strategies related to Arctic variability will need to focus primarily on regional mechanistic drivers operating on interannual and seasonal time-scales. We propose that this future decoupling of the Arctic from the North Pacific should be taken into consideration for long-term climate mitigation strategies related to the Arctic.

METHODS

Coupled model simulations

This study investigates the Arctic-North Pacific relationship using monthly data in two periods, namely, the historical (or present-day [PD]) and future simulations under Shared Socio-Economic Pathways (SSPs) provided by the Coupled Model Intercomparison Project Phase 6 (CMIP6[35]) and the CESM2 Large Ensemble Community Project (CESM2LE[34]). We use four SSP scenarios under the CMIP6 project, namely, SSP1-2.6, SSP2-4.5, SSP3-7.0, and SSP5-8.5, respectively. Since the future simulations (SSPs) were available for 86 years (2015–2100), we opted for the last 86 years (1929–2014) of PD for our comparison. After choosing the scenarios, we selected the common models available for the variables needed for this study. Altogether, there were 34 climate models available for the PD and four SSP scenarios, and one ensemble member from each of the models was used. The calculation of the CMIP6 multi-model mean was carried out by averaging each of the individual climate models and then estimating the ensemble mean. Further details on the CMIP6 climate models used in this study are given in the Supplementary Information. This study uses other Model Intercomparison Projects (MIP) contributing to the CMIP6 project, namely the DAMIP, PAMIP, and CFMIP, and an extended projection under SSP1-2.6 and SSP5-8.5 (CMIP6-ext) for the period 1850–2300. The number of climate models available for each of the MIPs is 34 (CMIP6), 4 (DAMIP), 4 (PAMIP), 9 (CFMIP), and 10 (CMIP6-ext), respectively. All the analysis presented in the study uses the same set of models for each of the MIPs. Further details on each of these MIPs are provided in the Supplementary Information.

The Community Earth System Model version 2 (CESM2) Large Ensemble (LE) project provides climate simulations for the period 1850–2100 under CMIP6 historical and SSP3-7.0 forcing scenarios. The output from the first 50 out of a total of 100 ensemble members was used. A total of 10 members were initialized through macro-perturbations, and four clusters of 10 members each were initialized with micro-perturbations[34]. The historical simulations (1850–2014) were initialized with pre-industrial conditions stemming from a spinup run of longer than 1000 years and projections over 2015–2100 following the SSP3-7.0 scenario in which the radiative forcing hits 7.0 W m^{-2} by 2100. The statistical mean of all the ensemble members is used to show the ensemble mean response. A more comprehensive description of the component models involved in CESM2LE is given in Supplementary Information.

Reanalysis dataset

To evaluate the CMIP6 and CESM2LE simulations, we utilized the NOAA/Cooperative Institute for Research in Environmental Sciences (CIRES) twentieth-century reanalysis product, version 3.0[52]. The NOAA/CIRES product is available at a horizontal resolution of 1° × 1° for the entire analysis period of the historical simulations (1929–2014; psl.noaa.gov/data/gridded/data.20th-C_ReanV3.html). For ease of comparison, we denote the reanalysis product as observations in this study. We chose the NOAA/CIRES reanalysis dataset owing to its coverage of all the necessary ocean, atmospheric, and sea-ice variables required for our study during the historical period. Furthermore, this long-term dataset cover the same time period as the CMIP6 historical data that we analyzed.

Methodology

The Arctic region in this study covers the entire domain poleward of 70°N and the Pacific sector of the Arctic and is chosen as the area bounded by 70°N–90°N, 90°E–90°W. We define the term 'difference' as the interannual change (relative to the previous year). Accordingly, a positive SAT difference during OND corresponds to an increase of the OND SAT compared to the OND SAT during the previous year. In this study, we denote the historical simulation for the period 1929–2014 as PD (present-day) and the future scenarios for the period 2015–2100 as SSPs. The forced variability is represented by the ensemble mean of all the climate models, whereas the residual (individual models minus the ensemble mean computed) represents the internal variability. The North Pacific Index (NPI)[32] is defined as the area-weighted average of SLP anomalies over the North Pacific Ocean bounded by 30°N–65°N, 160°E–140°W. But the spatial position of the dominant SLP variability in the North Pacific may vary in different datasets and under future projections. To take care of this shift in spatial position and to be consistent with the AL and NPO indices, we define the NPI difference in the study as the area-weighted average of the SLP difference over a larger spatial domain (20°N–70°N, 120°E–100°W).

DATA AVAILABILITY

All the data used in our study can be freely downloaded from the following sources. All the CMIP6 variables used in this study can be accessed at esgf-node.llnl.gov/search/cmip6. The CESM2LE data can be accessed at https://www.earthsystemgrid.org/dataset/ucar.cgd.cesm2le.output.html. The reanalysis products from NOAA/CIRES, available at psl.noaa.gov/data/gridded/data.20thC_ReanV3.html.

CODE AVAILABILITY

All codes are available upon request to the corresponding author.

REFERENCES

1. Moritz, R. E., Bitz, C. M. & Steig, E. J. Dynamics of recent climate change in the Arctic. *Science* **297**, 1497–1502 (2002).
2. Serreze, M. C., Barrett, A. P., Stroeve, J. C., Kindig, D. N. & Holland, M. M. The emergence of surface–based Arctic amplification. *Cryosphere* **3**, 11–19 (2009).
3. Serreze, M. C. & Barry, R. G. Processes and impacts of Arctic amplification: A research synthesis. *Glob. Planet. Change* **77**, 85–96 (2011).
4. Davy, R., Chen, L. & Hanna, E. Arctic amplification metrics. *Int. J. Climatol.* **38**, 4384–4394 (2018).
5. Dai, A., Luo, D., Song, M. & Liu, J. Arctic amplification is caused by sea-ice loss under increasing CO2. *Nat. Commun.* **10**, 121 (2019).
6. Stuecker, M. F. et al. Polar amplification dominated by local forcing and feed-backs. *Nat. Clim. Change* **8**, 1076–1081 (2018).
7. Chung, E. S. et al. Cold–season Arctic Amplification driven by Arctic Ocean-mediated seasonal energy transfer. *Earth's Future* **9**, e2020EF001898 (2021).
8. Overland, J. E. et al. Nonlinear response of mid-latitude weather to the changing Arctic. *Nat. Clim. Change* **6**, 992–999 (2016).
9. Dai, A. & Song, M. Little influence of Arctic amplification on mid-latitude climate. *Nat. Clim. Change* **10**, 231–237 (2020).
10. Liu, J., Curry, J. A., Wang, H., Song, M. & Horton, R. M. Impact of declining Arctic sea ice on winter snowfall. *Proc. Natl Acad. Sci. USA* **109**, 4074–4079 (2012).
11. Mori, M., Watanabe, M., Shiogama, H., Inoue, J. & Kimoto, M. Robust Arctic sea-ice influence on the frequent Eurasian cold winters in past decades. *Nat. Geosci.* **7**, 869–873 (2014).
12. Kug, J.-S. et al. Two distinct influences of Arctic warming on cold winters over North America and East Asia. *Nat. Geosci.* **8**, 759–762 (2015).
13. Kretschmer, M., Coumou, D., Donges, J. F. & Runge, J. Using causal effect net-works to analyze different Arctic drivers of midlatitude winter circulation. *J. Clim.* **29**, 4069–4081 (2016).
14. Cohen, J., Screen, J. A., Furtado, J. C. & Barlow, M. Recent Arctic amplification and extreme mid–latitude weather. *Nat. Geosci.* **7**, 627–637 (2014).
15. Francis, J. A. & Vavrus, S. J. Evidence for a wavier jet stream in response to rapid Arctic warming. *Environ. Res. Lett.* **10**, 014005 (2015).
16. Yeo, S.-R. et al. Recent climate variation in the Bering and Chukchi Seas and its linkages to large-scale circulation in the Pacific. *Clim. Dyn.* **42**, 2423–2437 (2014).
17. Screen, J. A. & Francis, J. A. Contribution of sea–ice loss to Arctic amplification is regulated by Pacific Ocean decadal variability. *Nat. Clim. Change* **6**, 856–860 (2016).
18. Clancy, R., Bitz, C. & Blanchard-Wrigglesworth, E. The influence of ENSO on Arctic sea ice in large ensembles and observations. *J. Clim.* **34**, 9585–9604 (2021).
19. Hamouda, M. E., Pasquero, C. & Tziperman, E. Decoupling of the Arctic Oscillation and North Atlantic Oscillation in a warmer climate. *Nat. Clim. Change* **11**, 137–142 (2021).
20. Chylek, P., Folland, C. K., Lesins, G., Dubey, M. K. & Wang, M. Arctic air temperature change amplification and the Atlantic multidecadal oscillation. *Geophys. Res. Lett.* **36**, L14801 (2009).
21. Zhang, J., Orsolini, Y. J., Limpasuvan, V. & Ukita, J. Impact of the Pacific sector sea ice loss on the sudden stratospheric warming characteristics. *npj Clim. Atmos. Sci.* **5**, 74 (2022).
22. Hwang, S.-O., Yeh, S.-W., Oh, S.-Y. & Lee, J. Recent weakening linkage between Arctic oscillation and Aleutian low during boreal winter and its impact on surface temperature over Eastern Eurasia. *Atmos. Sci. Lett.* **23**, e1089 (2022).
23. Wallace, J. M. & Gutzler, D. S. Teleconnections in the Geopotential Height Field during the Northern Hemisphere Winter. *Mon. Weather Rev.* **109**, 784–812 (1981).
24. Chen, S., Yu, B., Wu, R., Chen, W. & Song, L. The dominant North Pacific atmospheric circulation patterns and their relations to Pacific SSTs: historical simulations and future projections in the IPCC AR6 models. *Clim. Dyn.* **56**, 701–725 (2021).
25. Yu, J.-Y. & Kim, S. T. Relationships between extratropical sea level pressure variations and the central Pacific and eastern Pacific types of ENSO. *J. Clim.* **24**, 708–720 (2011).
26. Deser, C., Simpson, G. C., McKinnon, K. A. & Phillips, A. S. The Northern Hemisphere extratropical atmospheric circulation response to ENSO: How well do we know it and how do we evaluate models accordingly? *J. Clim.* **30**, 5059–5082 (2017).
27. Svendsen, L., Keenlyside, N., Bethke, I., Gao, Y. & Omrani, N. E. Pacific contribution to the early twentieth–century warming in the Arctic. *Nat. Clim. Change* **8**, 793–797 (2018).
28. Screen, J. A. & Deser, C. Pacific Ocean variability influences the time of emergence of a seasonally ice–free Arctic Ocean. *Geophys. Res. Lett.* **46**, 2222–2231 (2019).
29. Linkin, M. E. & Nigam, S. The North Pacific Oscillation–West Pacific Teleconnection Pattern: Mature-Phase Structure and Winter Impacts. *J. Clim.* **21**, 1979–1997 (2008).
30. Sung, M.-K. et al. Tropical influence on the North Pacific Oscillation drives winter extremes in North America. *Nat. Clim. Change* **9**, 413–418 (2019).
31. Kim, H. et al. Arctic Sea Ice Loss as a Potential Trigger for Central Pacific El Niño Events. *Geophys. Res. Lett.* **47**, e2020GL087028 (2020).
32. Trenberth, K. E. & Hurrell, J. W. Decadal atmospheric-ocean variations in the Pacific. *Clim. Dyn.* **9**, 303–319 (1994).
33. Ceballos, L. I., Di Lorenzo, E., Hoyos, C. D., Schneider, N. & Taguchi, B. North Pacific Gyre Oscillation synchronizes climate fluctuations in the eastern and western boundary systems. *J. Clim.* **22**, 5163–5174 (2009).
34. Rodgers, K. B. et al. Ubiquity of human-induced changes in climate variability. *Earth Syst. Dynam.* **12**, 1393–1411 (2021).
35. Eyring, V. et al. Overview of the Coupled Model Intercomparison Project Phase 6 (CMIP6) experimental design and organization. *Geosci. Model Dev.* **9**, 1937–1958 (2016).

36. Chapman, W. L. & Walsh, J. E. Simulations of Arctic Temperature and Pressure by Global Coupled Models. *J. Clim.* **40**, 609–632 (2007).

37. Stroeve, J. C. et al. Trends in Arctic sea ice extent from CMIP5, CMIP3 and observations. *Geophys. Res. Lett.* **39**, L16502 (2012).

38. Serreze, M. C. & Stroeve, J. Arctic sea ice trends, variability and implications for seasonal ice forecasting. *Philos. Trans. R. Soc. A* **373**, 20140159 (2015).

39. Alexander, M. et al. The atmospheric response to realistic Arctic sea ice anomalies in an AGCM during winter. *J. Clim.* **17**, 890–905 (2004).

40. Screen, J. A., Deser, C. & Simmonds, I. Local and remote controls on observed Arctic warming. *Geophys. Res. Lett.* **39**, L10709 (2012).

41. Gillett, N. P. et al. The Detection and Attribution Model Intercomparison Project (DAMIP v1.0)contribution to CMIP6. *Geosci. Model Dev.* **9**, 3685–3697 (2016).

42. Smith, D. M. et al. The Polar Amplification Model Intercomparison Project (PAMIP) contribution to CMIP6: investigating the causes and consequences of polar amplification. *Geosci. Model Dev.* **12**, 1139–1164 (2019).

43. Fang, C., Wu, L. & Zhang, X. The impact of global warming on the pacific decadal oscillation and the possible mechanism. *Adv. Atmos. Sci.* **31**, 118–130 (2014).

44. Li, S. et al. The Pacific Decadal Oscillation less predictable under greenhouse warming. *Nat. Clim. Chang.* **10**, 30–34 (2020).

45. Bonan, D. B. & Blanchard-Wrigglesworth, E. Nonstationary teleconnection between the Pacific Ocean and Arctic sea ice. *Geophys. Res. Lett.* **47**, e2019GL085666 (2020).

46. Webb, M. J. et al. The Cloud Feedback Model Intercomparison Project (CFMIP) contribution to CMIP6. *Geosci. Model Dev.* **10**, 359–384 (2017).

47. Ding, Q. et al. Tropical forcing of the recent rapid Arctic warming in northeastern Canada and Greenland. *Nature* **509**, 209–212 (2014).

48. Bader, J. The origin of regional Arctic warming. *Nature* **509**, 167–168 (2014).

49. Skific, N. & Francis, J. A. Drivers of projected change in Arctic moist static energy transport. *J. Geophys. Res.* **118**, 2748–2761 (2013).

50. Audette, A. et al. Opposite responses of the dry and moist eddy heat transport into the Arctic in the PAMIP experiments. *Geophys. Res. Lett.* **48**, e2020GL089990 (2021).

51. Song, S.-Y., Yeh, S.-W., Kim, H. & Holbrook, N. J. Arctic warming contributes to increase in Northeast Pacific marine heatwave days over the past decades. *Commun. Earth Environ.* **4**, 25 (2023).

52. Compo, G. P. et al. The Twentieth Century Reanalysis Project. *Q. J. R. Meteorol.* **137**, 1–28 (2011).

AUTHOR CONTRIBUTIONS

S.J. and K.-J.H. designed the study and wrote the paper. K.-J.H., C.L.E.F., S.-S.L., K.B.R., and D.E.L. were involved in the analysis and interpretation of the results. All authors contributed to the writing and revision of the paper.

COMPETING INTERESTS

The authors declare no competing interests.

ADDITIONAL INFORMATION

Supplementary information The online version contains supplementary material available at https://doi.org/10.1038/s41612-023-00480-6.

Correspondence and requests for materials should be addressed to Kyung-Ja Ha.

Reprints and permission information is available at http://www.nature.com/reprints

Publisher's note Springer Nature remains neutral with regard to jurisdictional claims in published maps and institutional affiliations.